

Graph Theoretical Analysis Reveals: Women’s Brains are Better Connected than Men’s

Balázs Szalkai^a, Bálint Varga^a, Vince Grolmusz^{a,b,*}

^a*PIT Bioinformatics Group, Eötvös University, H-1117 Budapest, Hungary*

^b*Uratim Ltd., H-1118 Budapest, Hungary*

Abstract

Deep graph-theoretic ideas in the context with the graph of the World Wide Web led to the definition of Google’s PageRank and the subsequent rise of the most-popular search engine to date. Brain graphs, or connectomes, are being widely explored today. We believe that non-trivial graph theoretic concepts, similarly as it happened in the case of the World Wide web, will lead to discoveries enlightening the structural and also the functional details of the animal and human brains. When scientists examine large networks of tens or hundreds of millions of vertices, only fast algorithms can be applied because of the size constraints. In the case of diffusion MRI-based structural human brain imaging, the effective vertex number of the connectomes, or brain graphs derived from the data is on the scale of several hundred today. That size facilitates applying strict mathematical graph theory algorithms even for some hard-to-compute (or NP-hard) quantities like set cover or balanced minimum cut.

In the present work we have examined brain graphs, computed from the data of the Human Connectome Project. Significant differences were found between the male and female structural brain graphs: we show that the average female connectome has more edges, has larger minimal bisection width, and has more spanning trees than the average male connectome. Since the average female brain weights less than the brain of males, these properties show that the female brain is more “well-connected” or perhaps, more “efficient” in a sense than the brain of males.

1. Introduction

In the last several years hundreds of publications appeared describing or analyzing structural or functional networks of the brain, frequently referred to as “connectome” [1, 2]. Some of these publications analyzed data from healthy

*Corresponding author

Email addresses: szalkai@pitgroup.org (Balázs Szalkai), varga@pitgroup.org (Bálint Varga), grolmusz@pitgroup.org (Vince Grolmusz)

humans [3, 4, 5, 6], and some compared the connectome of the healthy brain with diseased one [7, 8, 9, 10, 11].

So far, the analyses of the connectomes mostly used tools developed for very large networks, such as the graph of the World Wide Web (with billions of vertices), or protein-protein interaction networks (with tens or hundreds of thousands of vertices), and because of the huge size of original networks, these methods used only very fast algorithms and frequently just primary degree statistics and graph-edge counting between pre-defined regions or lobes of the brain [12].

In the present work we demonstrate that deep and more intricate graph theoretic parameters could also be computed by using, among other tools, contemporary integer programming approaches for connectomes with several hundred vertices.

With these mathematical tools we show statistically significant differences in some graph properties of the connectomes, computed from MRI imaging data of male and female brains. We will not try to associate behavioral patterns of males and females with the discovered structural differences [12] (see also the debate that article has generated: [13, 14, 15]), because we do not have behavioral data of the subjects of the imaging study, and, additionally, we cannot describe high-level functional properties implied by those structural differences. However, we clearly demonstrate that deep graph-theoretic parameters show "better" connections in a certain sense in female connectomes than in male ones.

The study of [12] analyzed the 95-vertex graphs of 949 subjects aged between 8 and 22 years, using edge-counting and basic statistics for the numbers of edges running either between or within different lobes of the brain (the parameters deducted were called *hemispheric connectivity ratio*, *modularity*, *transitivity* and *participation coefficients*, see [12] for the definitions). It was found that males have significantly more intra-hemispheric edges than females, while females have significantly more inter-hemispheric edges than males.

2. Results and Discussion

We have analyzed the connectomes of 96 subjects, 52 females and 44 males, each with 66, 120 and 250 node-resolutions, and each graphs with five different weight functions. We considered the connectomes as graphs with weighted edges, and performed graph-theoretic analyses with computing some polynomial-time computable and also some NP-hard graph parameters on the individual graphs, and then compared the results statistically for the male and the female group.

We have found that female connectomes have more edges, larger (normalized) minimum bisection widths and larger minimum-vertex covers and more spanning trees than the male connectomes.

In order to describe the parameters, significantly differing in male and female connectomes, we need to place them in the context of their graph theoretical definitions.

2.1. Edge number and edge weights

We have found significantly higher number of edges (counted with 5 types of weights and also without any weights) in both hemispheres and also in the whole brain in females, in all resolutions. This finding is surprising, since we used the same parcellation and the same tractography and the same graph-construction methods for female and male brains, and because it is proven that females have, on average, less-weighting brains than males [16]. For example, in the 250-vertex resolution, the average number of (unweighted) edges in female connectomes is 1826, in males 1742, with $p = 0.00063$. The work of [12] reported similar findings in inter-hemispheric connections only.

2.2. Minimum cut and balanced minimum cut

Suppose the nodes, or the vertices, of a graph are partitioned into two, disjoint, non-empty sets, say X and Y ; their union is the whole vertex-set of the graph. The X, Y cut is the set of *all* edges connecting vertices of X with the vertices of Y (Figure 1A). The size of the cut is the number of edges in the cut. In graph theory, the size of the minimum cut is an interesting quantity. The minimum cut between vertices a and b is the minimum cut, taken for all X and Y , where vertex a is in X and b is in Y . This quantity gives the “bottleneck”, in a sense, between those two nodes (c.f., Menger theorems and Ford-Fulkerson’s Min-Cut-Max-Flow theorem [17, 18]). The minimum cut in a graph is defined to be the cut with the fewest edges for *all* non-empty sets X and Y , partitioning the vertices.

Clearly, the size of the minimum cut in a non-connected graph is 0. Very frequently, however, in connected graphs, the minimum cut is determined by just the smallest degree node: that node is the only element of set X and all the other vertices of the graph are in Y (Figure 1B). Because of this phenomenon, minimum cut is frequently queried for the “balanced” case, when the size (i.e., the number of vertices) of X and Y needs to be equal (or, more exactly, may differ by at most one if the number of the vertices of the graph is odd), see Figure 1C. This problem is referred to as *the balanced minimum cut* or the *minimum bisection* problem. If the minimum bisection is small that means that there exist a partition of the vertices into two sets of equal size that are connected with only few edges. If the minimum bisection is large then the two half-sets in *every possible bisections* of the graph are connected by many edges.

Therefore, the balanced minimum cut of a graph is independent of the particular labeling of the nodes. The number of all the balanced cuts in a graph with n vertices is greater than

$$\frac{1}{n+1}2^n,$$

that is, for $n = 250$, this number is very close to the number of atoms in the visible universe [19]. Consequently, one cannot practically compute the minimum bisection width by reviewing all the bisections in a graph of that size. Moreover, the complexity of computing this quantity is known to be NP-hard

[20] in general, but with contemporary integral programming approaches, for the graph-sizes we are dealing with, the exact values are computable.

We show that within both hemispheres the minimum bisection size of female connectomes are significantly larger than the minimum bisection size of the males.

Moreover, we show that this remains true if we normalize with the edge-weights: that is, *this phenomenon cannot be due* to the higher number of edges or the greater edge weights in the female brain: it is an intrinsic property of the female brain graph.

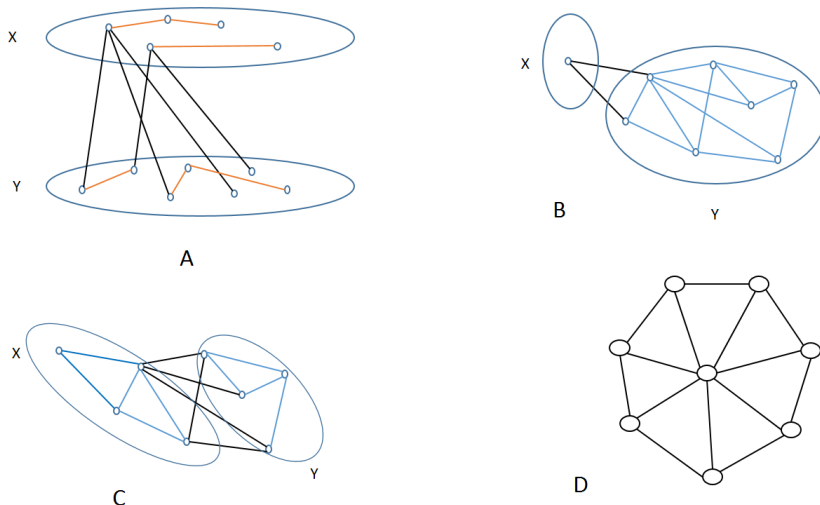


Figure 1: Panel A: An X-Y cut. The cut-edges are colored black. Panel B: An un-balanced minimum cut. Panel C: A balanced cut. Panel D: The wheel graph.

2.3. The number of spanning trees

A *tree* in graph theory is a connected, cycle-free graph. Any tree on n vertices has the same number of edges: $n - 1$. Trees, and tree-based structures are common in science: phylogenetic trees, hierarchical clusters, data-storage on hard-disks, or a computational model called *decision trees* all apply graph-theoretic trees. A *spanning tree* is a minimal subgraph of a connected graph that is still connected. Some graphs have no spanning trees at all: only connected graphs have spanning trees. A tree has only one spanning tree: itself. Any connected graph on n vertices has a minimum of $n - 1$ and a maximum of $n(n - 1)/2$ edges [21]. A connected graph with few edges still may have exponentially many different spanning trees: e.g., the n -vertex wheel on Figure 1D has at least 2^{n-1} spanning trees (for $n \geq 4$). Cayley's famous theorem, and its celebrated

proof with Prüfer codes [22] shows that the number of spanning trees of the complete graph on n vertices is n^{n-2} .

For graphs in general, one can compute the number of their spanning trees by Kirchoff's matrix tree theorem [23, 24] using the eigenvalues of the Laplacian matrix [24] of the graph.

We show that female connectomes have significantly higher number of spanning trees than the connectomes of males.

3. Materials and Methods

3.1. Data source and graph computation:

The dataset applied is a subset of the Human Connectome Project [25] anonymized 500 Subjects Release:

(<http://www.humanconnectome.org/documentation/S500>) of healthy subjects between 22 and 35 years of age. Data was downloaded in October, 2014. The Connectome Mapper Toolkit (<http://cmtk.org>) was applied for partitioning, tractography and the construction of the graphs. Lausanne2008 mapping [26] was used for creating the partitions into 66, 120 and 250 regions of interests (ROIs). Tractography was performed by choosing the deterministic streamline method. The graphs were constructed as follows: the nodes correspond to the ROIs in the specific resolution. Two nodes are connected by an edge if there exists at least one fiber (determined by the tractography step) connecting the ROIs, corresponding to the nodes.

The weights of the edges are computed by several methods, taking into account the lengths and the multiplicities of the fibers, connecting the nodes:

- **Unweighted:** Each edge has weight 1.
- **FiberN:** The number of fibers traced along the edge: this number is larger than one if more than one fibers connect two cortical areas, corresponding to the two endpoints of the edge.
- **FAMean:** The mean fractional anisotropy of the fibers, belonging to the edge.
- **FiberLengthMean:** The average length of the fibers, connecting the two endpoints of the edge.
- **FiberNDivLength:** The number of fibers, divided by their average length. This quantity is related to the simple electrical model of the nerve fibers: by modeling the fibers as electrical resistors with resistances proportional to the average fiber length, this quantity is precisely the conductance between the two regions of interest. Additionally, **FiberNDivLength** can be observed as a reliability measure of the edge: longer fibers are less reliable than the shorter ones, due to possible error accumulation in the tractography algorithm that constructs the fibers from the anisotropy

data. Multiple fibers connecting the same two cortical areas, corresponding to the endpoints, add to the reliability of the edge, because of the independent connections.

The matrices of the graphs were generalized to include the edge weights, that is, the “1” entries of the adjacency matrices were replaced by the weights of the corresponding edges, in each weighting method.

3.2. Graph parameters:

We wrote a C# program to analyze the connectome, computed from human diffusion MRI images. The program calculated various graph parameters for each brain graph, including:

- Number of edges (**Sum**)
- Normalized largest eigenvalue (**AdjLMaxDivD**): The largest eigenvalue of the adjacency matrix, divided by the average degree. Dividing by the average degree of vertices was necessary because the largest eigenvalue is bounded by the average and maximum degree and thus is considered by some a kind of “average degree” itself [?]. This means that a denser graph may have a bigger λ_{max} largest eigenvalue solely because of a larger average degree.
- Eigengap of the transition matrix (**PGEigengap**): The transition matrix P_G is obtained by dividing all the rows of the adjacency matrix by the degree of the corresponding node. When performing a random walk on the graph, for nodes i and j , the corresponding matrix element describes the probability of transitioning to node j , supposing that we are at node i . The eigengap of a matrix is the difference of the largest and the second largest eigenvalue. It has been linked to the conductance of a graph [?], which is a measure of how difficult it is to partition the graph into two parts with fewer than expected edges.
- Hoffman’s bound (**AdjOnePlusLMaxDivAbsLMin**): The expression

$$1 + \frac{\lambda_{max}}{|\lambda_{min}|},$$

where λ_{max} and λ_{min} denote the largest and smallest eigenvalues of the adjacency matrix. It is a lower bound for the chromatic number of the graph. The chromatic number should generally be higher for denser graphs, as the addition of an edge may make a previously valid coloring invalid.

- Logarithm of number of spanning trees (**LogAbsSpanningTreeN**): The number of spanning trees in a connected graph can be calculated from the spectrum of its Laplacian [23, 24]:

$$\frac{1}{n} \lambda_1 \lambda_2 \cdots \lambda_{n-1}.$$

Denser graphs tend to have more spanning trees, as the addition of an edge introduces zero or more new spanning trees.

- **Balanced minimum cut, divided by the number of edges (MinCutBalDivSum)**: The task is to partition the graph into two sets whose size may differ from each other by at most 1, so that the number of edges crossing the cut is minimal. This is the “balanced minimum cut” problem, or sometimes called the “minimum bisection width” problem. For a brain, we expected it to cut the graph along the boundary of the two hemispheres, which was indeed proved when we analyzed the results.
- **Minimum cost spanning tree (MinSpanningTree)**, calculated with Kruskal’s algorithm.
- **Minimum weighted vertex cover (MinVertexCover)**: Each vertex should have a (possibly fractional) weight assigned such that, for each edge, the sum of the weights of its two endpoints is at least 1. This is the fractional relaxation of the NP-hard vertex-cover problem [27]. The minimum of the sum of all vertex-weights is computable by a linear programming approach.
- **Minimum vertex cover (MinVertexCoverBinary)**: Same as above, but each weight must be 0 or 1. In other words, a minimum size set of vertices is selected such that each edge is covered by at least one of the selected vertices. This NP-hard graph-parameter is computed only for the unweighted case. The exact values are computed by an integer programming solver SCIP (<http://scip.zib.de>), [28, 29].

The above 9 parameters were computed for all three resolutions and for the left and the right hemispheres and also for the whole connectome, with all 5 weight functions (with the following exceptions: `MinVertexCoverBinary` was computed only for the unweighted case, and the `MinSpanningTree` was not computed for the unweighted case, because of the trivial result).

3.3. Statistical analysis

Each connectome was computed in multiple resolutions (33, 60, 125 nodes in each hemisphere: that is; 66, 120 and 250 nodes in the whole brain), we had three graphs for each brain. In addition, the parameters were calculated separately for the connectome within the left and right hemispheres as well, not only the whole graph, since we wanted to examine whether statistically significant differences can be attributed to only the left/right hemispheres. Each subjects’ brain was corresponded to 9 graphs (3 resolutions, each in the left and the right hemispheres, plus the whole cortex) and for each graph we calculated 9 parameters, each (with the exceptions noted above) with 5 different edge weights. This means that we assigned $7 \cdot 5 \cdot 3 + 1 \cdot 3 + 4 \cdot 3 = 120$ attributes to each resolution of the 96 brains, that is, 360 attributes to each brain.

The statistical null hypothesis [30] of ours was that the graph parameters do not differ between the male and the female groups. As the first approach, we have used ANOVA (Analysis of variance) [31] to assign p-values for all parameters in each hemispheres and in each resolutions and in each weight-assignments.

Our very large number of attributes may lead to false negatives, i.e., to “type II” statistical errors: in other words, it may happen that an attribute, with a very small p-value may appear “at random”, simply because we tested a lot of attributes. In order to deal with “type II” statistical errors, we followed the route described below.

We divided the population randomly into two sets by the parity of the sum of the digits in their ID. The first set was used for making hypotheses and the second set for testing these hypotheses. This was necessary to avoid type II errors resulting from multiple testing correction. If we made hypotheses for all the numerical parameters, then the Holm-Bonferroni correction [32] we used would have unnecessarily increased the p-values. Thus we needed to filter the hypotheses first, and that is why we needed the first set. Testing on the first set allowed us to reduce the number of hypotheses and test only a few of them on the second set.

The hypotheses were filtered by performing ANOVA (Analysis of variance) [31] on the first set. Only those hypotheses were selected to qualify for the second round where the p-value was less than 1%. The selected hypotheses were then tested for the second set as well, and the resulting p-value corrected with the Holm-Bonferroni correction method [32] with a significance level of 5%.

In Table 1 those hypotheses rejected were highlighted in bold, meaning that *all* the corresponding graph parameters differ significantly in sex groups at a combined significance level of 5%.

We also highlighted (in italic) those p-values which were individually less than the threshold, meaning that these hypotheses can *individually* be rejected at a level of 5%, but it is very likely that *not all* of these graph parameters are significantly different between the sexes.

4. Conclusions:

We have computed 66-, 120- and 250-vertex-graphs from the diffusion MRI images of the 96 subjects of 52 females and 44 males, between the age of 22 and 35. We have found, after a careful statistical analysis, significant differences between some graph theoretical parameters of the male and female brain graphs. Our findings show that the female brain graphs have generally more edges (counted with- and without weights), have larger normalized minimum bisection widths and have more spanning trees (counted with- and without weights) than the connectomes of males (Table 1). Additionally, with weaker statistical validity, some spectral properties and the minimum vertex cover also differ in the connectomes of different sexes (each with $p < 0.02$).

5. Data availability:

The unprocessed and pre-processed MRI data is available at the Human Connectome Project's website:

<http://www.humanconnectome.org/documentation/S500> [25].

Half-Scale	Property	p (1st)	p (2nd)	p (corrected)
60	Right_MinCutBalDivSum_FAMean	0.00807	<i>0.00003</i>	0.00368
33	All_LogAbsSpanningTreeN_FiberNDivLength	0.00003	<i>0.00004</i>	0.00417
33	Left_MinCutBalDivSum_FiberN	0.00403	<i>0.00011</i>	0.01212
33	Right_MinCutBalDivSum_FAMean	0.00496	<i>0.00015</i>	0.01625
33	All_Sum_Unweighted	0.00025	<i>0.00022</i>	0.02372
60	Left_MinCutBalDivSum_FiberN	0.00001	<i>0.00023</i>	0.02427
33	All_LogAbsSpanningTreeN_FiberN	0.00001	<i>0.00028</i>	0.02983
33	Right_Sum_FAMean	0.00028	<i>0.00029</i>	0.03050
125	All_Sum_Unweighted	0.00063	<i>0.00032</i>	0.03320
60	All_Sum_Unweighted	0.00026	<i>0.00042</i>	0.04352
125	All_Sum_FAMean	0.00014	<i>0.00047</i>	0.04755
60	All_LogAbsSpanningTreeN_FiberN	0.00000	<i>0.00048</i>	0.04849
33	All_Sum_FAMean	0.00029	<i>0.00050</i>	0.05010
60	Right_Sum_FAMean	0.00062	<i>0.00051</i>	0.05097
33	Left_Sum_Unweighted	0.00378	<i>0.00068</i>	0.06664
125	Right_Sum_FAMean	0.00085	<i>0.00084</i>	0.08119
125	Left_Sum_Unweighted	0.00293	<i>0.00092</i>	0.08843
60	All_Sum_FAMean	0.00015	<i>0.00097</i>	0.09260
125	Left_MinCutBalDivSum_FiberN	0.00002	<i>0.00108</i>	0.10109
33	Left_LogAbsSpanningTreeN_FiberNDivLength	0.00339	<i>0.00118</i>	0.10991
33	All_LogAbsSpanningTreeN_Unweighted	0.00114	<i>0.00123</i>	0.11273
125	Left_MinCutBalDivSum_FiberLengthMean	0.00411	<i>0.00123</i>	0.11156
33	All_LogAbsSpanningTreeN_FAMean	0.00012	<i>0.00126</i>	0.11352
33	Right_Sum_Unweighted	0.00019	<i>0.00128</i>	0.11380
60	Left_MinCutBalDivSum_Unweighted	0.00265	<i>0.00134</i>	0.11814
33	Left_MinCutBalDivSum_Unweighted	0.00206	<i>0.00136</i>	0.11827
125	All_LogAbsSpanningTreeN_FAMean	0.00043	<i>0.00150</i>	0.12901
60	Right_LogAbsSpanningTreeN_FAMean	0.00144	<i>0.00169</i>	0.14369
33	Left_MinCutBalDivSum_FiberNDivLength	0.00031	<i>0.00175</i>	0.14674
60	All_LogAbsSpanningTreeN_FiberNDivLength	0.00000	<i>0.00178</i>	0.14747
60	All_LogAbsSpanningTreeN_Unweighted	0.00219	<i>0.00183</i>	0.15016
60	Right_Sum_Unweighted	0.00068	<i>0.00186</i>	0.15045
60	All_LogAbsSpanningTreeN_FAMean	0.00019	<i>0.00211</i>	0.16906
125	Left_Sum_FAMean	0.00026	<i>0.00212</i>	0.16766
33	Right_LogAbsSpanningTreeN_FAMean	0.00068	<i>0.00238</i>	0.18603
60	Left_MinCutBalDivSum_FiberLengthMean	0.00892	<i>0.00245</i>	0.18840
33	Left_Sum_FAMean	0.00056	<i>0.00279</i>	0.21171
125	Left_MinCutBalDivSum_Unweighted	0.00154	<i>0.00289</i>	0.21644
125	Right_LogAbsSpanningTreeN_FAMean	0.00380	<i>0.00304</i>	0.22527
33	Left_LogAbsSpanningTreeN_FiberN	0.00012	<i>0.00407</i>	0.29307
60	Left_Sum_Unweighted	0.00232	<i>0.00456</i>	0.32374
33	Left_LogAbsSpanningTreeN_FAMean	0.00082	<i>0.00504</i>	0.35295
125	Right_MinCutBalDivSum_Unweighted	0.00462	<i>0.00543</i>	0.37453

33	Right_LogAbsSpanningTreeN_FiberNDivLength	0.00022	0.00582	0.39545
125	Left_LogAbsSpanningTreeN_FAMean	0.00060	0.00596	0.39947
60	Left_Sum_FAMean	0.00032	0.00660	0.43547
33	Left_AdjLMaxDivD_FiberN	0.00501	0.00804	0.52256
125	Right_Sum_Unweighted	0.00224	0.00845	0.54071
60	All_Sum_FiberN	0.00000	0.00938	0.59109
60	Right_MinCutBalDivSum_FiberN	0.00563	0.01101	0.68237
60	Right_MinCutBalDivSum_Unweighted	0.00492	0.01212	0.73922
60	Left_LogAbsSpanningTreeN_FAMean	0.00105	0.01226	0.73585
60	Left_LogAbsSpanningTreeN_FiberN	0.00014	0.01272	0.75040
33	All_Sum_FiberN	0.00000	0.01290	0.74797
125	All_Sum_FiberN	0.00000	0.01358	0.77381
33	Right_LogAbsSpanningTreeN_Unweighted	0.00547	0.01446	0.80974
60	Left_LogAbsSpanningTreeN_FiberNDivLength	0.00285	0.01455	0.80051
125	All_MinVertexCover_FAMean	0.00289	0.01713	0.92503
33	All_AdjOnePlusLMaxDivAbsLMin_FAMean	0.00087	0.02011	1.06569
33	All_Sum_FiberNDivLength	0.00002	0.02117	1.10102
125	Right_MinCutBalDivSum_FiberN	0.00234	0.02197	1.12032
33	Right_LogAbsSpanningTreeN_FiberN	0.00086	0.02560	1.28016
125	Right_MinCutBalDivSum_FiberLengthMean	0.00234	0.02663	1.30467
33	Right_MinCutBalDivSum_FiberNDivLength	0.00072	0.02854	1.36985
60	Left_MinCutBalDivSum_FiberNDivLength	0.00019	0.02897	1.36166
125	All_LogAbsSpanningTreeN_FiberN	0.00092	0.03315	1.52494
60	Right_MinCutBalDivSum_FiberLengthMean	0.00768	0.04500	2.02515
60	All_Sum_FiberNDivLength	0.00008	0.04728	2.03301
60	Right_LogAbsSpanningTreeN_FiberNDivLength	0.00051	0.04886	2.05197
125	All_LogAbsSpanningTreeN_FiberNDivLength	0.00106	0.05102	2.09181
60	Right_LogAbsSpanningTreeN_FiberN	0.00046	0.05585	2.23406
33	Right_MinCutBalDivSum_FiberN	0.00346	0.06284	2.45074
33	Right_AdjOnePlusLMaxDivAbsLMin_FiberNDivLength	0.00560	0.06309	2.39739
125	Left_MinCutBalDivSum_FiberNDivLength	0.00642	0.06548	2.42270
33	All_PGEigengap_FiberN	0.00941	0.06784	2.44232
125	Left_MinVertexCover_FAMean	0.00107	0.07139	2.49865
125	All_Sum_FiberNDivLength	0.00044	0.07318	2.48798
33	Right_Sum_FiberN	0.00000	0.07799	2.57379
33	Right_Sum_FiberNDivLength	0.00018	0.07920	2.53454
60	Left_Sum_FiberN	0.00000	0.08380	2.59777
60	Right_Sum_FiberN	0.00001	0.08653	2.59588
60	Left_AdjOnePlusLMaxDivAbsLMin_Unweighted	0.00848	0.08944	2.59364
33	Left_Sum_FiberN	0.00000	0.09430	2.54609
125	Left_Sum_FiberN	0.00040	0.11447	2.86183
60	Right_Sum_FiberNDivLength	0.00180	0.12102	2.90436
33	All_PGEigengap_FiberNDivLength	0.00122	0.15998	3.67964
125	Right_Sum_FiberN	0.00012	0.16411	3.61039
33	Left_Sum_FiberNDivLength	0.00043	0.16774	3.52254
60	Left_Sum_FiberNDivLength	0.00100	0.22542	4.28294
125	Right_Sum_FiberNDivLength	0.00562	0.23691	4.26443
125	All_PGEigengap_FiberNDivLength	0.00950	0.24879	4.22950
33	Right_AdjOnePlusLMaxDivAbsLMin_FAMean	0.00587	0.32069	5.13106
33	All_MinVertexCoverBinary_Unweighted	0.00716	0.38829	5.82431

125	Right_PGEigengap_FAMean	0.00023	0.39495	5.52930
125	Right_LogAbsSpanningTreeN_FiberNDivLength	0.00942	0.41026	5.33336
33	Left_AdjOnePlusLMaxDivAbsLMin_FiberN	0.00175	0.41913	5.02961
33	All_MinVertexCover_FiberNDivLength	0.00036	0.46677	5.13452
33	Right_MinSpanningTree_FiberLengthMean	0.00491	0.55239	4.97150
125	Right_MinSpanningTree_FiberLengthMean	0.00601	0.55631	4.45047
60	All_MinVertexCover_FiberN	0.00232	0.71406	3.57029
33	All_MinVertexCover_FiberN	0.00244	0.84437	1.68874
125	All_MinVertexCover_FiberN	0.00055	0.92958	0.92958

Table 1: The results and the statistical analysis of the graph-theoretical evaluation of the sex differences in the 96 diffusion MRI images. The first column gives the number of nodes in each hemisphere: the number of nodes in the whole graph is the double of that number. The second column describes the graph parameter computed: its syntactics is as follows: each parameter-name contains two separating “_” symbols that define three parts of the parameter-name. The first part describe the hemisphere or the whole connectome with the words Left, Right or All. The second part describes the parameter computed, and the third part the weight function used (their definitions are given in section “Materials and methods”). The third column contains the p-values of the first round, the second column the p-values of the second round, and the third column the (very strict) Holm-Bonferroni correction of the p-value. With $p=0.05$ *all* the first 12 rows describe significantly different graph theoretical properties between sexes. One-by-one, each row with italic third column describe significant differences between sexes, with $p=0.05$. For the details we refer to the section “Statistical analysis”.

6. Acknowledgments

The authors declare no conflicts of interest.

References

- [1] P. Hagmann, P. E. Grant, D. A. Fair, Mr connectomics: a conceptual framework for studying the developing brain., *Front Syst Neurosci* 6 (2012) 43. doi:10.3389/fnsys.2012.00043. URL <http://dx.doi.org/10.3389/fnsys.2012.00043>
- [2] R. C. Craddock, M. P. Milham, S. M. LaConte, Predicting intrinsic brain activity., *Neuroimage* 82 (2013) 127–136. doi:10.1016/j.neuroimage.2013.05.072. URL <http://dx.doi.org/10.1016/j.neuroimage.2013.05.072>
- [3] G. Ball, P. Aljabar, S. Zebari, N. Tusor, T. Arichi, N. Merchant, E. C. Robinson, E. Ogundipe, D. Rueckert, A. D. Edwards, S. J. Counsell, Rich-club organization of the newborn human brain., *Proc Natl Acad Sci U S A*

111 (20) (2014) 7456–7461. doi:10.1073/pnas.1324118111.
URL <http://dx.doi.org/10.1073/pnas.1324118111>

- [4] C. I. Bargmann, Beyond the connectome: how neuromodulators shape neural circuits., *Bioessays* 34 (6) (2012) 458–465. doi:10.1002/bies.201100185.
URL <http://dx.doi.org/10.1002/bies.201100185>
- [5] D. Batalle, E. Muñoz-Moreno, F. Figueras, N. Bargallo, E. Eixarch, E. Gratacos, Normalization of similarity-based individual brain networks from gray matter mri and its association with neurodevelopment in infants with intrauterine growth restriction., *Neuroimage* 83 (2013) 901–911. doi:10.1016/j.neuroimage.2013.07.045.
URL <http://dx.doi.org/10.1016/j.neuroimage.2013.07.045>
- [6] D. J. Graham, Routing in the brain., *Front Comput Neurosci* 8 (2014) 44. doi:10.3389/fncom.2014.00044.
URL <http://dx.doi.org/10.3389/fncom.2014.00044>
- [7] F. Agosta, S. Galantucci, P. Valsasina, E. Canu, A. Meani, A. Marcone, G. Magnani, A. Falini, G. Comi, M. Filippi, Disrupted brain connectome in semantic variant of primary progressive aphasia., *Neurobiol Aging*doi: 10.1016/j.neurobiolaging.2014.05.017.
URL <http://dx.doi.org/10.1016/j.neurobiolaging.2014.05.017>
- [8] A. F. Alexander-Bloch, P. T. Reiss, J. Rapoport, H. McAdams, J. N. Giedd, E. T. Bullmore, N. Gogtay, Abnormal cortical growth in schizophrenia targets normative modules of synchronized development., *Biol Psychiatry*doi:10.1016/j.biopsych.2014.02.010.
URL <http://dx.doi.org/10.1016/j.biopsych.2014.02.010>
- [9] J. T. Baker, A. J. Holmes, G. A. Masters, B. T. T. Yeo, F. Krienen, R. L. Buckner, D. Öngür, Disruption of cortical association networks in schizophrenia and psychotic bipolar disorder., *JAMA Psychiatry* 71 (2) (2014) 109–118. doi:10.1001/jamapsychiatry.2013.3469.
URL <http://dx.doi.org/10.1001/jamapsychiatry.2013.3469>
- [10] P. Besson, V. Dinkelacker, R. Valabregue, L. Thivard, X. Leclerc, M. Baulac, D. Sammler, O. Colliot, S. Lehericy, S. Samson, S. Dupont, Structural connectivity differences in left and right temporal lobe epilepsy., *Neuroimage* 100C (2014) 135–144. doi:10.1016/j.neuroimage.2014.04.071.
URL <http://dx.doi.org/10.1016/j.neuroimage.2014.04.071>
- [11] L. Bonilha, T. Nesland, C. Rorden, P. Fillmore, R. P. Ratnayake, J. Fridriksson, Mapping remote subcortical ramifications of injury after ischemic strokes., *Behav Neurol* 2014 (2014) 215380. doi:10.1155/2014/215380.
URL <http://dx.doi.org/10.1155/2014/215380>

- [12] M. Ingalhalikar, A. Smith, D. Parker, T. D. Satterthwaite, M. A. Elliott, K. Ruparel, H. Hakonarson, R. E. Gur, R. C. Gur, R. Verma, Sex differences in the structural connectome of the human brain., *Proc Natl Acad Sci U S A* 111 (2) (2014) 823–828. doi:10.1073/pnas.1316909110. URL <http://dx.doi.org/10.1073/pnas.1316909110>
- [13] D. Joel, R. Tarrasch, On the mis-presentation and misinterpretation of gender-related data: the case of ingalhalikar’s human connectome study., *Proc Natl Acad Sci U S A* 111 (6) (2014) E637. doi:10.1073/pnas.1323319111. URL <http://dx.doi.org/10.1073/pnas.1323319111>
- [14] M. Ingalhalikar, A. Smith, D. Parker, T. D. Satterthwaite, M. A. Elliott, K. Ruparel, H. Hakonarson, R. E. Gur, R. C. Gur, R. Verma, Reply to Joel and Tarrasch: On misreading and shooting the messenger., *Proc Natl Acad Sci U S A* 111 (6) (2014) E638.
- [15] C. Fine, Neuroscience. his brain, her brain?, *Science* 346 (6212) (2014) 915–916. doi:10.1126/science.1262061. URL <http://dx.doi.org/10.1126/science.1262061>
- [16] S. F. Witelson, H. Beresh, D. L. Kigar, Intelligence and brain size in 100 postmortem brains: sex, lateralization and age factors., *Brain* 129 (Pt 2) (2006) 386–398. doi:10.1093/brain/awh696. URL <http://dx.doi.org/10.1093/brain/awh696>
- [17] E. L. Lawler, *Combinatorial optimization: networks and matroids*, Courier Dover Publications, 1976.
- [18] L. R. Ford, D. R. Fulkerson, Maximal flow through a network, *Canadian Journal of Mathematics* 8 (3) (1956) 399–404.
- [19] P. Ade, N. Aghanim, C. Armitage-Caplan, M. Arnaud, M. Ashdown, F. Atrio-Barandela, J. Aumont, C. Baccigalupi, A. Banday, R. Barreiro, et al., Planck 2013 results. xvi. cosmological parameters, arXiv preprint arXiv:1303.5076.
- [20] M. R. Garey, D. S. Johnson, L. Stockmeyer, Some simplified np-complete graph problems, *Theoretical computer science* 1 (3) (1976) 237–267.
- [21] L. Lovász, *Combinatorial problems and exercises*, 2nd Edition, American Mathematical Society, 2007.
- [22] H. Prüfer, Neuer beweis eines satzes über permutationen, *Arch. Math. Phys* 27 (1918) 742–744.
- [23] G. Kirchhoff, über die Auflösung der Gleichungen, auf welche man bei der untersuchung der linearen verteilung galvanischer Ströme geführt wird, *Ann. Phys. Chem.* 72.

- [24] F. R. Chung, Spectral graph theory, Vol. 92, American Mathematical Soc., 1997.
- [25] J. A. McNab, B. L. Edlow, T. Witzel, S. Y. Huang, H. Bhat, K. Heberlein, T. Feiweier, K. Liu, B. Keil, J. Cohen-Adad, M. D. Tisdall, R. D. Folkerth, H. C. Kinney, L. L. Wald, The Human Connectome Project and beyond: initial applications of 300 mT/m gradients., *Neuroimage* 80 (2013) 234–245. doi:10.1016/j.neuroimage.2013.05.074.
URL <http://dx.doi.org/10.1016/j.neuroimage.2013.05.074>
- [26] P. Hagmann, L. Cammoun, X. Gigandet, R. Meuli, C. J. Honey, V. J. Wedeen, O. Sporns, Mapping the structural core of human cerebral cortex., *PLoS Biol* 6 (7) (2008) e159. doi:10.1371/journal.pbio.0060159.
URL <http://dx.doi.org/10.1371/journal.pbio.0060159>
- [27] D. S. Hochbaum, Approximation algorithms for the set covering and vertex cover problems, *SIAM Journal on computing* 11 (3) (1982) 555–556.
- [28] T. Achterberg, T. Berthold, T. Koch, K. Wolter, Constraint integer programming: A new approach to integrate cp and mip, in: *Integration of AI and OR techniques in constraint programming for combinatorial optimization problems*, Springer, 2008, pp. 6–20.
- [29] T. Achterberg, Scip: solving constraint integer programs, *Mathematical Programming Computation* 1 (1) (2009) 1–41.
- [30] P. G. Hoel, et al., *Introduction to mathematical statistics.*, Introduction to mathematical statistics. (2nd Ed).
- [31] T. H. Wonnacott, R. J. Wonnacott, *Introductory statistics*, Vol. 19690, Wiley New York, 1972.
- [32] S. Holm, A simple sequentially rejective multiple test procedure, *Scandinavian Journal of Statistics* (1979) 65–70.

Appendix

In this appendix we list the graph-theoretic parameters computed for the 66-, the 120- and the 250 vertex graphs separately, their arithmetic means in the male and female groups, and the corresponding p-values. The values in these tables contain the values corresponded to round 1 (see the “Statistical analysis” subsection in the main text.

The scales denoted are *the number of the nodes in each hemisphere*, i.e., the actual vertex-numbers are 66, 120 and 251, respectively.

The graph-parameters are defined in the caption of Table 1.

Significant differences ($p < 0.01$) are denoted with an asterisk.

Scale 33, round 1

Property	Female	Male	p-value
All_AdjLMaxDivD_FAMean	1.36008	1.37750	0.06806
All_AdjLMaxDivD_FiberLengthMean	1.44214	1.43602	0.72030
All_AdjLMaxDivD_FiberN	2.02416	2.10529	0.05606
All_AdjLMaxDivD_FiberNDivLength	1.84476	1.86864	0.41834
All_AdjLMaxDivD_Unweighted	1.26760	1.26456	0.63251
All_AdjOnePlusLMaxDivAbsLMin_FAMean	4.36096	4.18564	0.00087 *
All_AdjOnePlusLMaxDivAbsLMin_FiberLengthMean	3.21938	3.26552	0.33136
All_AdjOnePlusLMaxDivAbsLMin_FiberN	2.63525	2.55573	0.03144
All_AdjOnePlusLMaxDivAbsLMin_FiberNDivLength	2.51038	2.40550	0.01815
All_AdjOnePlusLMaxDivAbsLMin_Unweighted	4.55192	4.43931	0.04616
All_LogAbsSpanningTreeN_FAMean	110.68439	101.81623	0.00012 *
All_LogAbsSpanningTreeN_FiberLengthMean	456.58682	452.94414	0.18693
All_LogAbsSpanningTreeN_FiberN	397.52283	389.77821	0.00001 *
All_LogAbsSpanningTreeN_FiberNDivLength	148.01677	139.84220	0.00003 *
All_LogAbsSpanningTreeN_Unweighted	191.64584	187.83800	0.00114 *
All_MinCutBalDivSum_FAMean	0.00793	0.00474	0.14869
All_MinCutBalDivSum_FiberLengthMean	0.03115	0.02889	0.47008
All_MinCutBalDivSum_FiberN	0.02924	0.02711	0.34092
All_MinCutBalDivSum_FiberNDivLength	0.02868	0.02644	0.38768
All_MinCutBalDivSum_Unweighted	0.04001	0.03721	0.28887
All_MinSpanningTree_FAMean	19.78188	18.63722	0.02232
All_MinSpanningTree_FiberLengthMean	1096.37958	1112.97289	0.10506
All_MinSpanningTree_FiberN	99.53846	102.93333	0.14280
All_MinSpanningTree_FiberNDivLength	3.65548	3.66822	0.93669
All_MinVertexCoverBinary_Unweighted	59.80769	59.00000	0.00716 *
All_MinVertexCover_FAMean	18.73144	18.10619	0.01699
All_MinVertexCover_FiberLengthMean	2014.06431	1955.70824	0.37460
All_MinVertexCover_FiberN	2427.21154	2315.20000	0.00244 *
All_MinVertexCover_FiberNDivLength	110.25657	103.59777	0.00036 *
All_MinVertexCover_Unweighted	40.90385	41.00000	0.32897
All_PGEigengap_FAMean	0.04737	0.02605	0.08788
All_PGEigengap_FiberLengthMean	0.03096	0.00890	0.02478
All_PGEigengap_FiberN	0.02757	0.00353	0.00941 *
All_PGEigengap_FiberNDivLength	0.03432	0.00074	0.00122 *
All_PGEigengap_Unweighted	0.03965	0.02592	0.23902
All_Sum_FAMean	222.01291	201.02562	0.00029 *
All_Sum_FiberLengthMean	16845.33062	15792.24352	0.06219
All_Sum_FiberN	11261.65385	10237.13333	0.00000 *
All_Sum_FiberNDivLength	476.56342	433.37987	0.00002 *
All_Sum_Unweighted	567.07692	539.80000	0.00025 *
Left_AdjLMaxDivD_FAMean	1.33644	1.35216	0.15767
Left_AdjLMaxDivD_FiberLengthMean	1.40515	1.38890	0.32795
Left_AdjLMaxDivD_FiberN	1.90607	2.02087	0.00501 *
Left_AdjLMaxDivD_FiberNDivLength	1.71498	1.77482	0.07539
Left_AdjLMaxDivD_Unweighted	1.24027	1.23523	0.43598
Left_AdjOnePlusLMaxDivAbsLMin_FAMean	4.55406	4.38621	0.01297
Left_AdjOnePlusLMaxDivAbsLMin_FiberLengthMean	3.25098	3.28435	0.51250

Left_AdjOnePlusLMaxDivAbsLMin_FiberN	2.71430	2.61098	0.00175	*
Left_AdjOnePlusLMaxDivAbsLMin_FiberNDivLength	2.66652	2.59451	0.13782	
Left_AdjOnePlusLMaxDivAbsLMin_Unweighted	4.73205	4.57434	0.01379	
Left_LogAbsSpanningTreeN_FAMean	53.29745	48.82262	0.00082	*
Left_LogAbsSpanningTreeN_FiberLengthMean	229.62443	227.31547	0.18763	
Left_LogAbsSpanningTreeN_FiberN	199.27124	195.24299	0.00012	*
Left_LogAbsSpanningTreeN_FiberNDivLength	73.52849	69.82086	0.00339	*
Left_LogAbsSpanningTreeN_Unweighted	95.45473	93.38638	0.01381	
Left_MinCutBalDivSum_FAMean	0.00687	0.00320	0.17151	
Left_MinCutBalDivSum_FiberLengthMean	0.23438	0.21147	0.01779	
Left_MinCutBalDivSum_FiberN	0.13337	0.12011	0.00403	*
Left_MinCutBalDivSum_FiberNDivLength	0.11057	0.09321	0.00031	*
Left_MinCutBalDivSum_Unweighted	0.24513	0.22019	0.00206	*
Left_MinSpanningTree_FAMean	9.57924	9.06313	0.04242	
Left_MinSpanningTree_FiberLengthMean	561.47024	560.36391	0.87722	
Left_MinSpanningTree_FiberN	51.23077	53.73333	0.26795	
Left_MinSpanningTree_FiberNDivLength	1.82447	1.89521	0.62729	
Left_MinVertexCoverBinary_Unweighted	30.23077	29.73333	0.09601	
Left_MinVertexCover_FAMean	9.23616	8.88642	0.01371	
Left_MinVertexCover_FiberLengthMean	1064.27185	1027.73430	0.35926	
Left_MinVertexCover_FiberN	1158.21154	1143.46667	0.55321	
Left_MinVertexCover_FiberNDivLength	54.26322	51.17634	0.02122	
Left_MinVertexCover_Unweighted	20.80769	20.83333	0.75017	
Left_PGEigengap_FAMean	0.02610	0.02189	0.78469	
Left_PGEigengap_FiberLengthMean	0.00518	0.02101	0.29068	
Left_PGEigengap_FiberN	0.01462	0.02490	0.54848	
Left_PGEigengap_FiberNDivLength	0.00167	0.03412	0.01371	
Left_PGEigengap_Unweighted	0.03035	0.01716	0.37080	
Left_Sum_FAMean	106.64056	96.80731	0.00056	*
Left_Sum_FiberLengthMean	8629.73791	8122.82646	0.13250	
Left_Sum_FiberN	5514.61538	5049.73333	0.00000	*
Left_Sum_FiberNDivLength	233.06402	213.49323	0.00043	*
Left_Sum_Unweighted	282.50000	269.06667	0.00378	*
Right_AdjLMaxDivD_FAMean	1.32878	1.34242	0.14511	
Right_AdjLMaxDivD_FiberLengthMean	1.39672	1.38478	0.30191	
Right_AdjLMaxDivD_FiberN	2.00803	2.09048	0.05380	
Right_AdjLMaxDivD_FiberNDivLength	1.76990	1.81343	0.09784	
Right_AdjLMaxDivD_Unweighted	1.25268	1.24720	0.29540	
Right_AdjOnePlusLMaxDivAbsLMin_FAMean	4.47438	4.28666	0.00587	*
Right_AdjOnePlusLMaxDivAbsLMin_FiberLengthMean	3.33823	3.39478	0.29902	
Right_AdjOnePlusLMaxDivAbsLMin_FiberN	2.67311	2.57701	0.05411	
Right_AdjOnePlusLMaxDivAbsLMin_FiberNDivLength	2.62635	2.48983	0.00560	*
Right_AdjOnePlusLMaxDivAbsLMin_Unweighted	4.61480	4.50726	0.03806	
Right_LogAbsSpanningTreeN_FAMean	52.23541	48.12691	0.00068	*
Right_LogAbsSpanningTreeN_FiberLengthMean	218.23202	216.22757	0.16540	
Right_LogAbsSpanningTreeN_FiberN	190.60518	187.01436	0.00086	*
Right_LogAbsSpanningTreeN_FiberNDivLength	69.82171	66.16120	0.00022	*
Right_LogAbsSpanningTreeN_Unweighted	90.22281	88.49859	0.00547	*
Right_MinCutBalDivSum_FAMean	0.02476	0.00851	0.00496	*
Right_MinCutBalDivSum_FiberLengthMean	0.24577	0.22309	0.02216	
Right_MinCutBalDivSum_FiberN	0.13346	0.12050	0.00346	*
Right_MinCutBalDivSum_FiberNDivLength	0.10831	0.09357	0.00072	*
Right_MinCutBalDivSum_Unweighted	0.23713	0.22022	0.01629	
Right_MinSpanningTree_FAMean	10.30911	9.79708	0.10419	
Right_MinSpanningTree_FiberLengthMean	532.13580	547.85331	0.00491	*
Right_MinSpanningTree_FiberN	50.76923	52.53333	0.26282	
Right_MinSpanningTree_FiberNDivLength	1.94340	1.89232	0.58863	
Right_MinVertexCoverBinary_Unweighted	29.07692	28.73333	0.15457	
Right_MinVertexCover_FAMean	9.26572	9.03965	0.12382	
Right_MinVertexCover_FiberLengthMean	934.26071	897.95882	0.23661	
Right_MinVertexCover_FiberN	1169.63462	1122.93333	0.07986	
Right_MinVertexCover_FiberNDivLength	53.57144	51.50298	0.10452	
Right_MinVertexCover_Unweighted	20.11538	20.26667	0.10527	
Right_PGEigengap_FAMean	0.03374	0.02297	0.37001	
Right_PGEigengap_FiberLengthMean	0.03267	0.03079	0.89987	
Right_PGEigengap_FiberN	0.02779	0.02864	0.93906	
Right_PGEigengap_FiberNDivLength	0.00989	0.01439	0.72599	
Right_PGEigengap_Unweighted	0.03550	0.04237	0.59383	

Right_Sum_FAMean	105.62164	95.26436	0.00028	*
Right_Sum_FiberLengthMean	7644.90330	7086.91000	0.02974	
Right_Sum_FiberN	5378.03846	4884.66667	0.00000	*
Right_Sum_FiberNDivLength	225.94776	206.97587	0.00018	*
Right_Sum_Unweighted	261.30769	248.26667	0.00019	*

Scale 60, round 1

Property	Female	Male	p-value	
All_AdjLMaxDivD_FAMean	1.40519	1.42604	0.10040	
All_AdjLMaxDivD_FiberLengthMean	1.50483	1.50158	0.87806	
All_AdjLMaxDivD_FiberN	2.14552	2.22254	0.15242	
All_AdjLMaxDivD_FiberNDivLength	2.09783	2.04782	0.32031	
All_AdjLMaxDivD_Unweighted	1.30028	1.29097	0.27278	
All_AdjOnePlusLMaxDivAbsLMin_FAMean	4.40157	4.29660	0.02644	
All_AdjOnePlusLMaxDivAbsLMin_FiberLengthMean	3.19684	3.24689	0.32568	
All_AdjOnePlusLMaxDivAbsLMin_FiberN	2.50604	2.48884	0.64956	
All_AdjOnePlusLMaxDivAbsLMin_FiberNDivLength	2.34647	2.41938	0.07720	
All_AdjOnePlusLMaxDivAbsLMin_Unweighted	4.62935	4.51267	0.01233	
All_LogAbsSpanningTreeN_FAMean	194.36789	181.02797	0.00019	*
All_LogAbsSpanningTreeN_FiberLengthMean	739.78085	732.54400	0.09866	
All_LogAbsSpanningTreeN_FiberN	599.75641	588.60919	0.00000	*
All_LogAbsSpanningTreeN_FiberNDivLength	210.51276	200.74408	0.00000	*
All_LogAbsSpanningTreeN_Unweighted	322.08365	316.61840	0.00219	*
All_MinCutBalDivSum_FAMean	0.00668	0.00324	0.05930	
All_MinCutBalDivSum_FiberLengthMean	0.01706	0.01607	0.56293	
All_MinCutBalDivSum_FiberN	0.02658	0.02429	0.26627	
All_MinCutBalDivSum_FiberNDivLength	0.02495	0.02258	0.30029	
All_MinCutBalDivSum_Unweighted	0.02218	0.02065	0.30082	
All_MinSpanningTree_FAMean	30.14746	28.58509	0.02073	
All_MinSpanningTree_FiberLengthMean	1642.68263	1664.23693	0.07510	
All_MinSpanningTree_FiberN	140.23077	140.93333	0.55077	
All_MinSpanningTree_FiberNDivLength	4.42401	4.43795	0.92181	
All_MinVertexCoverBinary_Unweighted	96.46154	96.26667	0.66793	
All_MinVertexCover_FAMean	29.56250	28.72424	0.02181	
All_MinVertexCover_FiberLengthMean	3230.07900	3121.21684	0.29100	
All_MinVertexCover_FiberN	2444.92308	2337.40000	0.00232	*
All_MinVertexCover_FiberNDivLength	120.18766	116.22553	0.02502	
All_MinVertexCover_Unweighted	63.88462	63.96667	0.35805	
All_PGEigengap_FAMean	0.04227	0.02776	0.15347	
All_PGEigengap_FiberLengthMean	0.02753	0.01818	0.31327	
All_PGEigengap_FiberN	0.03835	0.01394	0.01448	
All_PGEigengap_FiberNDivLength	0.03415	0.02322	0.34495	
All_PGEigengap_Unweighted	0.03760	0.02061	0.13858	
All_Sum_FAMean	397.68878	360.50850	0.00015	*
All_Sum_FiberLengthMean	30670.09535	28478.19852	0.03582	
All_Sum_FiberN	12375.61538	11458.13333	0.00000	*
All_Sum_FiberNDivLength	548.61301	510.71378	0.00008	*
All_Sum_Unweighted	1020.80769	972.86667	0.00026	*
Left_AdjLMaxDivD_FAMean	1.37823	1.39812	0.12792	
Left_AdjLMaxDivD_FiberLengthMean	1.43638	1.42179	0.36739	
Left_AdjLMaxDivD_FiberN	1.84672	1.92762	0.12247	
Left_AdjLMaxDivD_FiberNDivLength	1.77313	1.80979	0.33521	
Left_AdjLMaxDivD_Unweighted	1.26380	1.25501	0.16858	
Left_AdjOnePlusLMaxDivAbsLMin_FAMean	4.57539	4.44885	0.01512	
Left_AdjOnePlusLMaxDivAbsLMin_FiberLengthMean	3.23550	3.25088	0.77158	
Left_AdjOnePlusLMaxDivAbsLMin_FiberN	2.80373	2.74220	0.14090	
Left_AdjOnePlusLMaxDivAbsLMin_FiberNDivLength	2.70077	2.64308	0.21782	
Left_AdjOnePlusLMaxDivAbsLMin_Unweighted	4.75280	4.61941	0.00848	*
Left_LogAbsSpanningTreeN_FAMean	96.10463	89.24791	0.00105	*
Left_LogAbsSpanningTreeN_FiberLengthMean	373.08820	368.64753	0.08834	
Left_LogAbsSpanningTreeN_FiberN	300.77077	295.82215	0.00014	*
Left_LogAbsSpanningTreeN_FiberNDivLength	105.00667	100.80255	0.00285	*
Left_LogAbsSpanningTreeN_Unweighted	162.00706	158.87197	0.01330	
Left_MinCutBalDivSum_FAMean	0.00873	0.00273	0.05683	
Left_MinCutBalDivSum_FiberLengthMean	0.19822	0.17378	0.00892	*
Left_MinCutBalDivSum_FiberN	0.12848	0.10467	0.00001	*

Left_MinCutBalDivSum_FiberNDivLength	0.06926	0.05546	0.00019	*
Left_MinCutBalDivSum_Unweighted	0.19535	0.17339	0.00265	*
Left_MinSpanningTree_FAMean	14.57467	13.88500	0.06189	
Left_MinSpanningTree_FiberLengthMean	828.34729	834.54850	0.36946	
Left_MinSpanningTree_FiberN	69.30769	72.20000	0.02902	
Left_MinSpanningTree_FiberNDivLength	2.16989	2.25626	0.53695	
Left_MinVertexCoverBinary_Unweighted	48.76923	48.86667	0.69355	
Left_MinVertexCover_FAMean	14.65360	14.09857	0.01273	
Left_MinVertexCover_FiberLengthMean	1700.29684	1637.18742	0.30481	
Left_MinVertexCover_FiberN	1169.82692	1125.20000	0.06266	
Left_MinVertexCover_FiberNDivLength	58.76113	56.23736	0.06303	
Left_MinVertexCover_Unweighted	32.28846	32.30000	0.88865	
Left_PGEigengap_FAMean	0.01961	0.02190	0.86455	
Left_PGEigengap_FiberLengthMean	0.02216	0.00139	0.02394	
Left_PGEigengap_FiberN	0.00575	0.04009	0.05929	
Left_PGEigengap_FiberNDivLength	0.02048	0.02131	0.96314	
Left_PGEigengap_Unweighted	0.01543	0.02920	0.25462	
Left_Sum_FAMean	197.41850	178.80563	0.00032	*
Left_Sum_FiberLengthMean	16079.40944	14931.40760	0.07487	
Left_Sum_FiberN	6071.96154	5641.93333	0.00000	*
Left_Sum_FiberNDivLength	269.09760	251.40080	0.00100	*
Left_Sum_Unweighted	519.53846	492.86667	0.00232	*
Right_AdjLMaxDivD_FAMean	1.35746	1.36837	0.36353	
Right_AdjLMaxDivD_FiberLengthMean	1.42015	1.41129	0.54264	
Right_AdjLMaxDivD_FiberN	2.05564	2.19134	0.01338	
Right_AdjLMaxDivD_FiberNDivLength	1.82146	1.86716	0.20816	
Right_AdjLMaxDivD_Unweighted	1.26684	1.25522	0.12057	
Right_AdjOnePlusLMaxDivAbsLMin_FAMean	4.37886	4.29574	0.20294	
Right_AdjOnePlusLMaxDivAbsLMin_FiberLengthMean	3.32686	3.36662	0.49418	
Right_AdjOnePlusLMaxDivAbsLMin_FiberN	2.66511	2.56838	0.01727	
Right_AdjOnePlusLMaxDivAbsLMin_FiberNDivLength	2.68679	2.59830	0.01992	
Right_AdjOnePlusLMaxDivAbsLMin_Unweighted	4.60861	4.51407	0.08448	
Right_LogAbsSpanningTreeN_FAMean	93.40566	87.27244	0.00144	*
Right_LogAbsSpanningTreeN_FiberLengthMean	357.99339	354.72404	0.14311	
Right_LogAbsSpanningTreeN_FiberN	291.07225	285.71190	0.00046	*
Right_LogAbsSpanningTreeN_FiberNDivLength	100.73228	96.21945	0.00051	*
Right_LogAbsSpanningTreeN_Unweighted	154.35405	151.95439	0.01162	
Right_MinCutBalDivSum_FAMean	0.02361	0.01005	0.00807	*
Right_MinCutBalDivSum_FiberLengthMean	0.20000	0.17303	0.00768	*
Right_MinCutBalDivSum_FiberN	0.11452	0.10111	0.00563	*
Right_MinCutBalDivSum_FiberNDivLength	0.06865	0.06326	0.09375	
Right_MinCutBalDivSum_Unweighted	0.19180	0.16911	0.00492	*
Right_MinSpanningTree_FAMean	15.61479	14.88977	0.06537	
Right_MinSpanningTree_FiberLengthMean	808.14079	824.37649	0.03729	
Right_MinSpanningTree_FiberN	70.46154	68.93333	0.07096	
Right_MinSpanningTree_FiberNDivLength	2.32813	2.26810	0.46298	
Right_MinVertexCoverBinary_Unweighted	47.34615	47.00000	0.29760	
Right_MinVertexCover_FAMean	14.70648	14.40974	0.13709	
Right_MinVertexCover_FiberLengthMean	1516.99670	1461.52391	0.23679	
Right_MinVertexCover_FiberN	1175.50000	1166.36667	0.68666	
Right_MinVertexCover_FiberNDivLength	59.59421	58.78162	0.47843	
Right_MinVertexCover_Unweighted	31.61538	31.73333	0.20363	
Right_PGEigengap_FAMean	0.04321	0.04336	0.98964	
Right_PGEigengap_FiberLengthMean	0.01221	0.01065	0.89437	
Right_PGEigengap_FiberN	0.02921	0.02958	0.96880	
Right_PGEigengap_FiberNDivLength	0.03730	0.02079	0.26831	
Right_PGEigengap_Unweighted	0.03612	0.02516	0.33929	
Right_Sum_FAMean	190.48228	172.48988	0.00062	*
Right_Sum_FiberLengthMean	13952.01182	13003.32443	0.04620	
Right_Sum_FiberN	5935.73077	5525.26667	0.00001	*
Right_Sum_FiberNDivLength	262.31420	246.32048	0.00180	*
Right_Sum_Unweighted	477.38462	454.86667	0.00068	*

Scale 125, round 1

Property	Female	Male	p-value
All_AdjLMaxDivD_FAMean	1.59824	1.62177	0.20251

All_AdjLMaxDivD_FiberLengthMean	1.72504	1.73145	0.81358	
All_AdjLMaxDivD_FiberN	3.00790	2.99029	0.82198	
All_AdjLMaxDivD_FiberNDivLength	3.06003	2.88353	0.06518	
All_AdjLMaxDivD_Unweighted	1.44314	1.43766	0.65566	
All_AdjOnePlusLMaxDivAbsLMin_FAMean	4.11594	4.07125	0.25943	
All_AdjOnePlusLMaxDivAbsLMin_FiberLengthMean	3.09745	3.17400	0.10768	
All_AdjOnePlusLMaxDivAbsLMin_FiberN	2.33189	2.36477	0.36494	
All_AdjOnePlusLMaxDivAbsLMin_FiberNDivLength	2.24918	2.30019	0.09467	
All_AdjOnePlusLMaxDivAbsLMin_Unweighted	4.26449	4.22883	0.31200	
All_LogAbsSpanningTreeN_FAMean	333.12470	309.35956	0.00043	*
All_LogAbsSpanningTreeN_FiberLengthMean	1319.41128	1305.87909	0.09485	
All_LogAbsSpanningTreeN_FiberN	958.25885	942.50363	0.00092	*
All_LogAbsSpanningTreeN_FiberNDivLength	261.95417	250.78296	0.00106	*
All_LogAbsSpanningTreeN_Unweighted	575.69057	565.47613	0.01073	
All_MinCutBalDivSum_FAMean	0.00258	0.00069	0.03188	
All_MinCutBalDivSum_FiberLengthMean	0.01055	0.00997	0.56364	
All_MinCutBalDivSum_FiberN	0.02503	0.02259	0.20939	
All_MinCutBalDivSum_FiberNDivLength	0.02020	0.01710	0.03711	
All_MinCutBalDivSum_Unweighted	0.01316	0.01222	0.25998	
All_MinSpanningTree_FAMean	51.00196	48.57885	0.01194	
All_MinSpanningTree_FiberLengthMean	2804.74772	2831.83990	0.06357	
All_MinSpanningTree_FiberN	245.92308	245.00000	0.53375	
All_MinSpanningTree_FiberNDivLength	7.99545	7.91594	0.74227	
All_MinVertexCoverBinary_Unweighted	166.65385	165.40000	0.14781	
All_MinVertexCover_FAMean	51.98307	50.16832	0.00289	*
All_MinVertexCover_FiberLengthMean	5248.81515	5090.58422	0.34139	
All_MinVertexCover_FiberN	2430.57692	2326.23333	0.00055	*
All_MinVertexCover_FiberNDivLength	127.46338	125.41222	0.14913	
All_MinVertexCover_Unweighted	116.23077	116.26667	0.79591	
All_PGEigengap_FAMean	0.02082	0.01471	0.41444	
All_PGEigengap_FiberLengthMean	0.01427	0.01011	0.49579	
All_PGEigengap_FiberN	0.00738	0.00600	0.74803	
All_PGEigengap_FiberNDivLength	0.01660	0.00046	0.00950	*
All_PGEigengap_Unweighted	0.02294	0.01989	0.71963	
All_Sum_FAMean	689.73851	628.62387	0.00014	*
All_Sum_FiberLengthMean	51558.63408	48397.55225	0.05764	
All_Sum_FiberN	13267.88462	12438.86667	0.00000	*
All_Sum_FiberNDivLength	618.33865	586.27221	0.00044	*
All_Sum_Unweighted	1826.03846	1742.66667	0.00063	*
Left_AdjLMaxDivD_FAMean	1.58597	1.61184	0.19191	
Left_AdjLMaxDivD_FiberLengthMean	1.67378	1.67488	0.96164	
Left_AdjLMaxDivD_FiberN	2.51455	2.59709	0.24706	
Left_AdjLMaxDivD_FiberNDivLength	2.46008	2.44949	0.86194	
Left_AdjLMaxDivD_Unweighted	1.42058	1.41216	0.45842	
Left_AdjOnePlusLMaxDivAbsLMin_FAMean	4.19268	4.14961	0.31372	
Left_AdjOnePlusLMaxDivAbsLMin_FiberLengthMean	3.12191	3.15801	0.48134	
Left_AdjOnePlusLMaxDivAbsLMin_FiberN	2.63594	2.59362	0.26584	
Left_AdjOnePlusLMaxDivAbsLMin_FiberNDivLength	2.52966	2.50832	0.61082	
Left_AdjOnePlusLMaxDivAbsLMin_Unweighted	4.35117	4.29447	0.14153	
Left_LogAbsSpanningTreeN_FAMean	164.44058	151.95998	0.00060	*
Left_LogAbsSpanningTreeN_FiberLengthMean	670.02502	661.91347	0.08436	
Left_LogAbsSpanningTreeN_FiberN	484.09662	477.60359	0.02239	
Left_LogAbsSpanningTreeN_FiberNDivLength	130.53137	126.33062	0.07742	
Left_LogAbsSpanningTreeN_Unweighted	290.55413	285.57630	0.03119	
Left_MinCutBalDivSum_FAMean	0.00188	0.00000	0.01777	
Left_MinCutBalDivSum_FiberLengthMean	0.14735	0.12215	0.00411	*
Left_MinCutBalDivSum_FiberN	0.10539	0.08507	0.00002	*
Left_MinCutBalDivSum_FiberNDivLength	0.02918	0.02209	0.00642	*
Left_MinCutBalDivSum_Unweighted	0.14392	0.12444	0.00154	*
Left_MinSpanningTree_FAMean	25.10810	23.82569	0.01171	
Left_MinSpanningTree_FiberLengthMean	1431.81175	1435.42334	0.67083	
Left_MinSpanningTree_FiberN	126.92308	126.06667	0.61065	
Left_MinSpanningTree_FiberNDivLength	4.18418	4.03231	0.41157	
Left_MinVertexCoverBinary_Unweighted	84.00000	83.20000	0.15412	
Left_MinVertexCover_FAMean	25.89765	24.77675	0.00107	*
Left_MinVertexCover_FiberLengthMean	2746.38841	2650.87601	0.30587	
Left_MinVertexCover_FiberN	1197.30769	1175.86667	0.33225	
Left_MinVertexCover_FiberNDivLength	65.03508	64.53534	0.69540	

Left_MinVertexCover_Unweighted	59.15385	59.13333	0.87392	
Left_PGEigengap_FAMean	0.02374	0.01735	0.47241	
Left_PGEigengap_FiberLengthMean	0.00270	0.01021	0.28459	
Left_PGEigengap_FiberN	0.00233	0.02003	0.01585	
Left_PGEigengap_FiberNDivLength	0.01115	0.02290	0.10359	
Left_PGEigengap_Unweighted	0.01192	0.00716	0.62088	
Left_Sum_FAMean	341.86488	310.44231	0.00026	*
Left_Sum_FiberLengthMean	26855.84149	24971.13564	0.06460	
Left_Sum_FiberN	6551.88462	6204.20000	0.00040	*
Left_Sum_FiberNDivLength	306.39045	293.36221	0.01442	
Left_Sum_Unweighted	926.34615	881.53333	0.00293	*
Right_AdjLMaxDivD_FAMean	1.51832	1.54700	0.12507	
Right_AdjLMaxDivD_FiberLengthMean	1.61182	1.62906	0.37469	
Right_AdjLMaxDivD_FiberN	2.57025	2.75485	0.02819	
Right_AdjLMaxDivD_FiberNDivLength	2.34753	2.37750	0.61484	
Right_AdjLMaxDivD_Unweighted	1.39063	1.39160	0.92921	
Right_AdjOnePlusLMaxDivAbsLMin_FAMean	4.12472	4.11339	0.81603	
Right_AdjOnePlusLMaxDivAbsLMin_FiberLengthMean	3.21816	3.32010	0.04777	
Right_AdjOnePlusLMaxDivAbsLMin_FiberN	2.54183	2.48873	0.06857	
Right_AdjOnePlusLMaxDivAbsLMin_FiberNDivLength	2.55201	2.50267	0.17018	
Right_AdjOnePlusLMaxDivAbsLMin_Unweighted	4.31441	4.30433	0.78744	
Right_LogAbsSpanningTreeN_FAMean	163.63973	152.83716	0.00380	*
Right_LogAbsSpanningTreeN_FiberLengthMean	640.51600	635.22698	0.18042	
Right_LogAbsSpanningTreeN_FiberN	465.96919	459.02995	0.01285	
Right_LogAbsSpanningTreeN_FiberNDivLength	126.60276	120.66424	0.00942	*
Right_LogAbsSpanningTreeN_Unweighted	279.19653	274.71948	0.03171	
Right_MinCutBalDivSum_FAMean	0.00959	0.00322	0.03000	
Right_MinCutBalDivSum_FiberLengthMean	0.14992	0.12148	0.00234	*
Right_MinCutBalDivSum_FiberN	0.10001	0.08633	0.00234	*
Right_MinCutBalDivSum_FiberNDivLength	0.03193	0.02816	0.14205	
Right_MinCutBalDivSum_Unweighted	0.13748	0.11683	0.00462	*
Right_MinSpanningTree_FAMean	25.95958	24.86484	0.05085	
Right_MinSpanningTree_FiberLengthMean	1367.27500	1390.89912	0.00601	*
Right_MinSpanningTree_FiberN	119.19231	118.86667	0.70146	
Right_MinSpanningTree_FiberNDivLength	3.93775	3.96494	0.81094	
Right_MinVertexCoverBinary_Unweighted	82.30769	81.66667	0.20770	
Right_MinVertexCover_FAMean	25.90289	25.23516	0.03478	
Right_MinVertexCover_FiberLengthMean	2485.78834	2418.73395	0.39406	
Right_MinVertexCover_FiberN	1128.59615	1112.30000	0.37231	
Right_MinVertexCover_FiberNDivLength	60.30418	59.94168	0.76940	
Right_MinVertexCover_Unweighted	57.07692	57.16667	0.40299	
Right_PGEigengap_FAMean	0.03969	0.00387	0.00023	*
Right_PGEigengap_FiberLengthMean	0.01512	0.01680	0.83123	
Right_PGEigengap_FiberN	0.02021	0.00234	0.02107	
Right_PGEigengap_FiberNDivLength	0.02041	0.01571	0.54656	
Right_PGEigengap_Unweighted	0.04484	0.03102	0.20379	
Right_Sum_FAMean	337.74022	308.44201	0.00085	*
Right_Sum_FiberLengthMean	24086.28238	22847.27016	0.12171	
Right_Sum_FiberN	6343.42308	5974.26667	0.00012	*
Right_Sum_FiberNDivLength	294.65559	280.13740	0.00562	*
Right_Sum_Unweighted	874.00000	835.60000	0.00224	*